

AN INTEGRATED APPROACH FOR THE DETERMINATION OF PERMEABILITY TENSORS AND SIMULATION OF NATURALLY FRACTURED RESERVOIRS

A. Gupta
The University of Missouri-Rolla

ABSTRACT

The use of permeability tensors is required for modeling fluid flow in anisotropic and heterogeneous reservoirs that present multiple zones of directional permeability or those categorized as naturally fractured reservoirs. A general procedure for characterizing complex reservoirs by integrating data and methods from different disciplines, and utilizing the permeability tensor is presented. Permeability tensors for geologically defined fracture patterns are derived, and these small-scale descriptors are incorporated into a reservoir simulation program capable of handling full tensor permeabilities. A series of numerical experiments are designed and conducted to observe what would be the influence, over a typical waterflood process in terms of fluid distribution and water break-through times, when variations to the properties that define the permeability tensor are introduced. A correct definition of the geometry and the permeability tensor distribution of the fracture system results in a more accurate reservoir simulation model.

INTRODUCTION

Substantial research has been conducted in the areas of geosciences and engineering in order to characterize naturally fractured reservoirs. Geoscientists have focused their research towards understanding the process of fracturing (rock mechanics) and the subsequent description of fracture characteristics such as density and orientation. Engineers have focused their attention to the description of the fluid flow in the fracture systems and in the development of accurate models (reservoir simulators), to reproduce the history and predict the hydrocarbon production for these complex systems. One of the most important factor that has been identified as a necessary addition to improve the overall description of such complex reservoirs is the definition of a nine-component permeability tensor for the fracture system. This tensor is used to model fluid flow in complex reservoirs with multiple zones of directional permeability, where the orientation and magnitude of the principal permeabilities may vary between different zones in the reservoir. This study incorporates current technology (seismic, well log and well test data) in the description of the fracture system, in order to define a realistic permeability tensor, that does not depend on random variables approximation and which can be properly incorporated in a naturally fractured reservoir simulation model.

DESCRIPTION OF METHOD

The equation of motion or Darcy's law that describes laminar single-phase fluid flow in a naturally fractured media is:

$$\bar{u} = -\frac{\bar{K}}{\mu} \nabla \Phi \tag{1}$$

where the flow potential, $\nabla \Phi$, is represented as⁶¹

$$\nabla \Phi = \nabla p + \rho \nabla h - \rho \frac{\partial \bar{u}}{\partial t} \tag{2}$$

and the permeability tensor is defined as:

$$\bar{K} = |K| \left[\bar{K} \right] \tag{3}$$

Eq. 3 states that the permeability tensor for a fracture media, called Snow's-tensor, is composed of two parts. The unit

permeability tensor, $[\bar{\bar{K}}]$, accounts for the directional effects in the fluid flow due to the existence of a fracture (or set of fractures) in the media. The permeability scalar, $|K|$, accounts for the intensity of the anisotropy that the fracture brings to the porous media. Permeability tensor is calculated based on the information about the fracture system that current technology is capable of providing. Mathematical details of the procedures to obtain permeability tensor can be found elsewhere. In this paper, some techniques to estimate the parameters involved in the unit permeability tensor calculation are discussed. Existing methods to obtain fracture directions (dip/strike) can be classified in two main groups. The first group is based on seismic data interpretation, in which after appropriate data processing, dip direction is estimated. The second group relies on well logging measurements to compute both fracture dip orientation and dip angle. Different techniques have been developed to estimate fracture direction from seismic data depending on the type of data set that is available. The main types of analysis are: (a) Shear waves studies of multi-component seismic data, (b) P-S converted wave, and, (c) P-wave studies^[7]. Shear wave studies take into account the effect of splitting experienced by a shear wave that propagates through an anisotropic medium^[8]. Even though multi-component surveys have been verified to be effective in delineating fracture strike, high acquisition and processing cost, limited availability of S-wave sources, and volume/quality of S-waves restricts their applicability. The rotational analysis of P-S converted waves is an alternative method^[9]. It has several advantages over the multi-component data. P-S waves are believed to contain the same information as shear waves by using compressional sources and therefore their acquisition is less expensive. P-wave data is the most commonly acquired seismic data. Two techniques have been used to estimate fracture orientation using existing P-wave data. It was shown that amplitude-variation-with-offset (AVO) response of P-waves can be affected by the presence of fractures depending on the relative orientation of the fractures and the recording line^[10]. Another technique based on P-wave recordings is the normal-move-out (NMO) analysis of multi-azimuth P-wave data^[11]. Wellbore imaging tools such as the formation micro-scanner (FMS) have also been used to estimate the dip direction of a fracture. It must be pointed out that scale and resolution for seismic based and well-log based estimates are quite different. Multi-well analysis along with geostatistical methods allows comparison of fracture attributes based on well-logs to the seismic based estimates.

PERMEABILITY TENSOR CALIBRATION

To obtain a representative tensor for the field, the following procedure is recommended on a well-by-well basis:

1. Pressure transient data for the well is collected.
2. Using the permeability tensor obtained from the method presented in the preceding, a simulation run is performed to model the pressure response of the well.
3. Field and model pressure derivative responses are compared in a log-log plot of pressure and time.
4. The permeability scalar is adjusted until an optimum match is obtained between the field and model pressure response.
5. Having a matched permeability scalar, a final and representative permeability tensor is defined through the use of Eq. (3).

It is important to notice that only the scalar portion of the permeability tensor is modified in the calibration procedure, since a single well pressure response is expected to be insensitive to the fracture orientation. The unit permeability tensor may be adjusted based on multi-well interference tests.

NUMERICAL EXPERIMENTS

This paper presents a series of numerical experiments that were designed and conducted to observe sensitivity, over a typical watertlood process (in terms of fluid distribution and water break-through times), to variations in parameters that define the permeability tensor.

The mathematical flow model developed by Evans and Guo^[15] and later programmed by Nacornthap^[38] to characterize the fluid flow phenomenon in naturally fractured reservoirs was selected as the basis of the simulator used to perform the numerical experiments in this study.

The simulator treats a fractured reservoir as a double porosity medium consisting of a heterogeneous, isotropic primary rock matrix and an anisotropic, heterogeneous fracture system. The distribution in space and orientation of the fracture is expressed in terms of the fracture permeability tensor. It allows flow through the rock matrix and the fracture to be described simultaneously. The fluid interaction terms coupling flow between the rock matrix and fracture, the gravity effects, the capillary forces and the fracture velocity of fluids are all taken into consideration. The presence or absence of fractures at any point in the reservoir system, as well as the orientation and anisotropy of fractures can be accounted

for by manipulating elements in the permeability tensor.

The simulator is able to handle simultaneous flow of three fluid phases: gas, oil, and water. A simplified black oil is used in this study, assuming that no mass transfer occurs between the water phase, and the gas and oil phases. In summary the main characteristics and assumptions with regard to the mathematical model were.

1. The reservoir treated as a double porosity medium; one porosity associated with the rock matrix and the second porosity associated with the fractures.
2. The rock is an elastic incompressible solid, and the changes in the rock matrix and fracture porosities are due to reordering and/or reorientation of the rock grains.
3. The primary rock matrix is isotropic and heterogeneous, whereas the fractures are anisotropic and heterogeneous.
4. Fluid velocities in both the primary pores and the fractures were assumed to be small such that the system exhibits laminar flow.
5. Primary rock matrix pore volume is independent of fracture pressure and the fracture pore volume is independent of matrix pressure.

A total of six numerical experiments are presented:

- a) To verify two general assumptions that are usually applied in naturally fractured reservoir studies when the fracture system is being characterized, i.e.: a) all fractures can be considered to be vertical when dealing with deep reservoirs, and, b) the fracture system orientation can be effectively reproduced through the application of a normal random distribution function for orientation. These assumptions are tested in the Dip Angle Case and Random Case, respectively.
- b) To determine if the geophysical data analysis concerning fracture orientation can be used with confidence towards the definition of the unit permeability tensor. Assuming that the belief of the geoscientists that the orientation of fractures can be predicted within an accuracy of ± 20 degrees is correct, the influence of this margin of error over a waterflood field application is described in the Dip Direction Case of this chapter.
- c) To test the sensitivity of the permeability scalar to its parameters. The influences that the variation of fracture aperture and fracture density has over the results of a waterflood scenario are tested in the Less Aperture, More Aperture and Fracture Density cases, respectively.

In all cases, a waterflood displacement of oil by water was used as the field application, selecting the difference in water break-through times observed in each case as the principal variable to be measured and compared, together with the final fluid saturation distribution in the field. The influence that each tensor property has over the resulting permeability tensors will be obtained. In order to be able to analyze and compare the intended cases, it was necessary to create a base case that served as the benchmark to which results of the remaining cases were compared. Any significant deviation from this base case will indicate a high influence of the parameter being analyzed.

To build the simulation run file, data from the paper of Thomas et al [39] was adapted. A reservoir section between an injection and production well was modeled using a $15' \times 15' \times 1$ grid system as shown in Fig.-1, with grid block dimension equal to 100 ft, for X and Y and 50 ft. for Z. The rock matrix permeability and porosity are set equal to 0.1 md and 0.15, while the fracture permeability is described by the permeability tensor, with porosity equal to 0.01. In the rock matrix as well as the fracture, the initial reservoir pressure is set at 4214.7 psia., with initial saturations of 0.88 for the oil, 0.12 for the water and 0.0 for the gas. The bubble point pressure is 1714.7 psia. The injection well and the production well are located at the blocks $1' \times 1' \times 1$ and $15' \times 15' \times 1$ respectively, as shown in Fig. 1. They are both set to a constant rate control, injecting 645 STB/D and producing 400 STB/D. The individual block fracture orientations are assumed to be known from seismic interpretation. Water-oil relative permeability and capillary pressure data are presented in Table 1.

For the base case it was assumed that all the tensor-defining properties were already known through the use of seismic and well log analysis as described previously. To simplify further tests, the fractures were assumed vertical with dip angle equal to ninety degrees.

Dip Angle Variation: The objective of this test was to verify if fractures can be assumed vertical in hydrocarbons accumulations studies and obtain the same response as when the actual dip angle information for fractures was available. All permeability tensor parameters are kept the same with the exception of the fracture dip angles that are varied from a lower limit of sixty degrees to an upper limit of seventy-five degrees with respect of the X-Y plane. The upper

limit restriction was set to a point (75°) so that fractures would preserve their natural dip angle, but will not be close enough to the ninety degrees that vertical fractures present. The lower limit restriction was not set less than 60° , because even in shallow reservoirs it is very difficult to find fractures that have a horizontal tendency. Fig. 2 shows the angle interval between which the fractures were allowed to oscillate with respect of a vertical fracture.

Random Dip Direction Variation: The objective of this test was to verify if fracture orientation can effectively be reproduced by a random normal distribution. Following the commonly used assumption that fracture system orientation (dip direction) may be reproduced by a normal probability distribution, the fracture orientation in each individual block was randomly generated. The result was a completely different grid fracture orientation than the one shown in Fig. 1, as presented in Fig. 3.

Dip Direction Variation: The objective of this test was to verify if the margin of error ($\pm 20^\circ$) that was generated in the definition of the fractures orientation from seismic interpretation would produce a significant variation over the results obtained in the base case simulation. All the permeability tensor properties were kept identical, but in order to determine the influence of fracture orientation on a flood performance, the fractures dip direction (orientation) were allowed to vary by ± 20 degrees from the data defined in the base case. A representation of the range of variation allowed for a single fracture is shown in Fig. 4.

Aperture Variation: All the permeability tensor properties were kept identical with the exception of the fracture aperture (W_f). In the permeability scalar definition the fracture aperture is raised to the third power, implying that any variation of aperture should produce significant changes in the resulting permeability tensor. However, it is desirable to observe how significant an influence this property variation represents. For this purpose, two cases were considered, in the first case the aperture was lowered from its original value of 0.005 inches to 0.001 inches, and in the second case it was increased to 0.01 inches. **Fracture Density Variation:** The objective of this case was to observe the sensitivity of the reservoir displacement behavior to variations in fracture density. This is also one of the more difficult parameters to determine. Increments up to three hundred percent were introduced to the original fracture density specified in the base case. Table 2, summarizes all the variations introduced to the base case, in order to effectively observe the sensitivity of fluid distribution and water break-through, to the variations in fracture system parameters.

DISCUSSION OF RESULTS

In this section, the results from the numerical experiments described previously are discussed, analyzed, and compared to the Base Case scenario on the basis of water break-through times, fluid saturation distribution and water-oil ratio.

Base Case: This case serves as the reference to which the other numerical experiments are compared. The water saturation distribution obtained at 500 and 1000 days of injection are presented in Figs. 5 and 6. It is observed that no water break-through has occurred at 500 days (Fig. 5) but occurs at 900 days, based on water production results. The cumulative water produced at 1000 days is 5.0 MSTB with a 0.58 water-oil ratio.

Dip Angle Variation: Figures 7 and 8 present the water saturation distribution after the dip angle modifications. From these two figures it is observed that a very slight modification in the overall water saturation distribution occurs around the field with respect of the base case. The water break-through, cumulative water and WOR at 1000 days are almost the same as for base case. This indicates that fractures in deep reservoirs may be assumed vertical without producing significant effect on the overall fluid displacement and distribution in the field.

Random Dip Direction Variation: Figures 9 and 10 present the water distribution for random fracture orientation. Figures 9 and 10 present a completely different scenario of water saturation distribution for the field, when compared with the base case at both 500 and 1000 days. This together with an earlier water break-through of 793 days and a WOR of 0.41 indicates that when fractures orientations are randomly generated the final solution may be significantly incorrect!

Dip Direction Variation: Figures 11 and 12 present the water saturation distribution after dip direction variations of ± 20 degrees. When comparing the above figures with the base case results, it was seen that no significant variation is observed in the field wide water saturation distribution, water break-through occurs nearly at the same time as in the base case, while the cumulative water production is the same (5.0 MSTB) and the WOR is 0.63. These results allow us to conclude that the fracture orientation data provided by seismic interpretation can be used with confidence in naturally fractured reservoir characterization studies, because the $\pm 20^\circ$ of uncertainty that this data possesses does not affect the general fluid behavior and distribution in the reservoir.

Aperture Variation: When fracture apertures were changed to 0.001 inches and 0.01 inches, significant variations are observed in the fluid saturation distribution. When the fracture aperture is reduced compared to the base case, the effect is so significant that no water break-through was detected up to 1000 days of injection. For the case of fracture aperture greater than base case, the break through happens earlier, after 842 days of injection, which is a 6.4% difference. For the larger aperture, the cumulative production increased by 100% to a total of 10 MSTB, with a final WOR of 0.65. It

can be concluded that, any variation of the fracture aperture produces a significant effect in the resulting permeability tensors and consequently over the general fluid displacement and distribution of a naturally fractured field.

Fracture Density Variation: A water saturation distribution very similar to the base case was observed when the fracture density was varied from the base case. Water break-through occurred only 16 days earlier than the base case, and the cumulative water production was increased almost 90% (9.0 MSTB), with a similar WOR of 0.60. These results were reached when the fracture density was incremented by 300%. For increments of 25%, 50%, 100% and 200% no noticeable variations in break-through time or cumulative water production was observed. The reason for such insensitivity of results to fracture density is that fracture constitute only a small fraction of the overall porosity and results suggest that it would require variations of the order of 300% in fracture densities to notice any significant change on the reservoir displacement performance. Figs. 13 – 14 and Table 3 show how all the scenarios reviewed present, in general, a very similar behavior, which allowed the verification or rejection of the general assumptions that are being reviewed and illustrated how big an impact the parameters defining the permeability tensor (aperture and fracture density cases) may have over the final results obtained in a field simulation.

CONCLUSIONS

A convenient procedure is presented to calculate and calibrate permeability tensors for highly anisotropic reservoirs. The proposed method combines a variety of data sources and tools such as well logging, well testing and seismic. Although a high degree of uncertainty is still involved in the estimation of the fracture system properties, it is possible to obtain permeability tensors (through calibration or history match) that are able to reproduce well and field history data. Advances in logging tools and seismic interpretation, tend to reduce the need for the use of random variables to statistically generate and characterize fracture networks. On the basis of the numerical experiments, it is possible to conclude that:

- a) It is reasonable to assume vertical fractures during the characterization of naturally fractured reservoirs.
- b) Geophysical data analysis can be used satisfactorily for the definition of the fracture orientation.
- d) The fracture aperture, at least for the permeability tensor definition being used in this thesis, has the greatest influence over the fluid displacement performance.
- e) Very high variations in fracture densities are needed to reflect a significant influence over the displacement results obtained (saturation, break through, etc.).

REFERENCES

- [1] Sterns, D.W. "Fracture as a Mechanism of Flow in Naturally Deformed Layered Rocks", Conference on Research in Tectonics Proc. Canada Geology Survey. Paper 68-52, pp 79-96. 1969.
- [2] Nelson, R.A. "Geologic Analysis of Naturally Fractured Reservoirs". Gulf Publishing Co, Houston, 1985.
- [3] Sterns, D.W. and Friedman, M. "Reservoirs in Fractured Rocks". AAPG, Tulsa, OK, Memoir 16, pp 82-10, 1972.
- [4] Aguilera, R. "Naturally Fractured Reservoirs". PennWell Publishing Company. 2nd Edition, 1995.
- [5] Sterns, D.W. "Macrofracture Patterns on Teton Anticline, Northwest Montana". American Geophysics Union Transcripts, pp 107-115, 1964.
- [6] Warren, J.E. and Root, P.J. "The Behavior of Naturally Fractured Reservoirs". Soc. Pet. Eng. J. Sept. 1963.
- [7] Odeh, A.S. "Unsteady-State Behavior of Naturally Fractured Reservoirs". SPE paper. 1964.
- [8] Warren, J.E. and Root, P.J. "Discussion", SPEJ, pp 64-66. 1964.
- [9] Da Prat Giovanni, Cinco-Ley Heber and Ramey Jr. Henry. "Decline Curve Analysis Using Type Curves for Two-Porosity Systems". SPE paper 9292. 1981.
- [10] Goode, P.A. and Thambynayagam, R.K.M. "Pressure Drawdown and Buildup Analysis of Horizontal Wells in Anisotropic Media". SPE paper 14250. 1985.
- [11] Daviau, F., Mouronval, G., Bourdarot, G. and Curutchet, P. "Pressure Analysis for Horizontal Wells". SPE paper 14251. 1985.
- [12] Rosa, A.J. and Carvalho, R.S. "A Mathematical Model for Pressure Evaluation in an Infinite Conductivity Horizontal Well". SPE paper 15967. 1987.
- [13] Rosa, A.J. and Carvalho, R.S. "Transient Pressure Behavior for Horizontal Wells in Naturally Fractured Reservoirs". SPE paper 18302. 1988
- [14] Aguilera, R. and Ng, M.C. "Transient Pressure Analysis of Horizontal Wells in Anisotropic Naturally Fractured Reservoirs". SPEFE, pp 95-100. March, 1991.
- [15] Guo, G. and Evans, R. "An Economic Model for Assessing the Feasibility of Exploiting Naturally Fractured Reservoirs by Horizontal Well Technology". SPE paper 26676. 1993.
- [16] Parsons, R.W. "Permeability of Idealized Fractured Rock". SPE paper 1289. 1966.
- [17] Snow, David T. "Anisotropic Permeability of Fractured Media". Water Resources Research, Vol. 5, NO. 6,

pp 1273-1289. December 1969.

[18] Snow, David T. "The Frequency and Apertures of Fractures in Rock". *Int. j. Rock Mech. Min. Sci.* Vol.7, pp 23-40. 1970.

[19] Long, J.C.S., Remer, J.S., and Witherspoon, P.A. "Porous Media Equivalents for Networks of Discontinuous Fractures". *Water Resources Research*, Vol.18, NO. 3, pp 645-658. June 1982.

[20] Long, J., Gilmour, P., and Witherspoon, P. "A Model for Steady Fluid Flow in Random Three-Dimensional Networks of Disc-Shaped Fractures". *Water Resources Research*, Vol.21, NO. 8, pp 1105-1115. August 1985.

[21] Leung, W.F. "A Tensor Model for Anisotropic and Heterogeneous Reservoirs with Variable Directional Permeabilities". SPE paper 15134. 1986.

[22] Kasap, E., and Lake, L. "Calculating the Effective Permeability Tensor of a Gridblock". SPE paper 18434. 1990.

[23] Kasap, E., Aasum, Y. and Kelkar, M. "Analytical Upscaling of Small-Scale Permeability Using a Full Tensor". SPE paper 25913. 1993.

[24] Kasap, E., Lee, J. and Kelkar, M. "Analytical Upscaling of Permeability for 3D Gridblocks". SPE paper 27875. 1996.

[25] Kasap, E., Soerawinata, T. and Kelkar, M. "Permeability Upscaling for Near-Wellbore Heterogeneities". SPE paper 36518. 1997.

[26] Lee, S.H., Durlofsky, L.J., Lough, M.F. and Chen, W.H. "Finite Difference Simulation of Geologically Complex Reservoirs with Tensor Permeabilities". SPE paper 38002. 1997.

[27] Durlofsky, L.J. "Numerical Calculation of Equivalent Grid Block Permeability Tensors for Heterogeneous Porous Media". *Water Resources Research*, Vol.27, NO.5, pp 699-708. May 1991.

[28] Durlofsky, L.J., Behrens, R.A., Jones, R.C. and Bernath, A. "Scale Up of Heterogeneous Three Dimensional Reservoir Descriptions". SPE paper 30709-P. 1996.

[29] Perez, M., Grechka, V. and Michelena R. "Fracture Detection In a Carbonate Reservoir Using a Variety of Seismic Methods," *Geophysics*, Vol. 64, No. 4, pp 1266-1276. 1999.

[30] Li, X-Y, and Mueller, M. "Case Studies of Multicomponent Data for Fracture Characterization: Austin Chalk Examples". *Carbonate Seismology, Geophysical Developments*. No 6. Chapter 14. 1997.

[31] Atta, E., and Michelena, R.J. "Mapping Distribution of Fractures In a Reservoir With P-S Converted Waves," *The Leading Edge*, 12, pp 664-676. 1995.

[32] Perez, M. Gibson, R. and Tksoz, N. "Detection of Fracture Orientation From Azimuthal Variation of P-wave AVO Responses," *Geophysics*, Vol. 64, No. 4, pp 1253-1265, 1999.

[33] Corrigan, D., Withers, R., Darnall, J., and Skopinski, T. "Analysis of Amplitude Versus Offset to Detect Gas-Oil Contacts in the Arabian Gulf," 66th Ann. Internat. Mtg., Soc. Expl. Geophys., Expanded Abstract, pp1834-1837. 1996.

[34] Oda, M. "Permeability Tensor for Discontinuous Rock Masses". *Geotechnique* 35, No. 4, pp 483-495. 1985.

[35] Bourdet, D and Gringarten, A.C. "Determination of Fissure Volume and Block Size in Fractured Reservoirs by Type-Curve Analysis" .SPE paper 9293. 1980.

[36] Lee, Jaedong. Ph.D Dissertation. "Analytical Upscaling of Permeabilities for reservoir Simulation Grid Blocks". University of Tulsa. 1996.

[37] Aasum, Y. Ph.D Dissertation. "Effective Properties of Reservoir simulator Grid Blocks". University of Tulsa. 1992.

[38] Nakornthap, K. Ph.D Dissertation. "Numerical Simulation of Multiphase Fluid Flow in Naturally Fractured Reservoirs". University of Oklahoma. 1982.

[39] Thomas, L.K., Dixon, T.N. and Pierson, R.G. "Fractured Reservoir Simulation". SPE paper 9305. 1982

ACKNOWLEDGMENT

Author would like to acknowledge the support from the University of Oklahoma and the U.S.D.O.E. research contract DE-AC26-99BC15212 titled "Development of Reservoir Characterization Techniques and Production Models for Exploiting Naturally Fractured.

NOMENCLATURE

K = permeability (L²), md.
 q = flow rate (L³/T). STB/D
 p = pressure (F/L²), psi.
 u = darcy velocity (L/T), ft/s.
 $\hat{\mu}$ = fluid viscosity (F-T/L²), cp.
 A = fluid density (M/L³), gr/cc.
 O = flow potential (F/L²)
 W_f = fracture aperture (L), ft.
 H = sample line (L), ft.
 B_o = oil formation factor (L³/L³), RB/STB.
 C_t = total compressibility (L²/F), psi⁻¹.
 = Porosity fraction.
 h = formation thickness (L), ft.
 r_w = wellbore radius (L), ft.
 C_{ij} = Mass fraction of component i in phase j
 g = acceleration of gravity
 x, y, z = Rectangular coordinantes
 \tilde{A} = Fluid interaction term between the fracture and the rock matix

Table 1
Water-Oil Relative and Capillary Pressure Data

S_w	K_{rw}	K_{row}	P_{cow} (PSI)	DS_w/DP_c (PSI ⁻¹)
0.0	0.0	1.00	214.0	-0.00122
0.20	0.01	0.834	50.00	-0.00122
0.30	0.02	0.723	2.00	-0.00714
0.40	0.03	0.492	0.0	-0.10000
0.50	0.06	0.304	-1.20	-0.06250
0.60	0.11	0.154	-4.00	-0.03570
0.70	0.18	0.042	-10.00	-0.01670
1.00	1.00	0.0	-190.00	-0.00167

Table 2
Description of Numerical Experiments

	Dip Direction	Dip Angle	Aperture	Frac. Number (N)
Base Case	All known	90° → Vertical	0.005 inch	100
Dip Direction	± 20° of base case	90° → Vertical	0.005 inch	100
Random D.D.	Random	90° → Vertical	0.005 inch	100
Dip. Angle	Same as base case	60° < δ < 75°	0.005 inch	100
More Aperture	Same as base case	90° → Vertical	0.010 inch	100
Less Aperture	Same as base case	90° → Vertical	0.0001 inch	100
Frac.Density	Same as base case	90° → Vertical	0.005 inch	400

Table 3
Results of Numerical Experiments

	Break Through (days)	Cumulative Water @ 1000 days (MSTB)	Cumulative Oil @ 1000 days (MMSTB)	WOR @ 1000 days (fraction)
Base Case	900	5.0	0.41	0.58
Dip Angle	903	5.3	0.40	0.67
Random D.D.	793	4.1*	0.36*	0.41*
Dip Direction	902	5.0	0.40	0.63
More Aperture	842	10	0.41	0.65
Less Aperture	Doesn't happen	0.0	0.40	0
Frac.Density	884	9.0	0.41	0.60

Note: (*) values recorded at 900 days

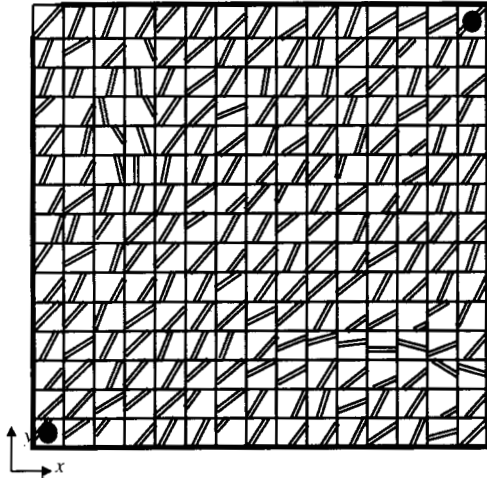


Figure 1 - Simulation Grid, with Fracture Orientation and Well Location

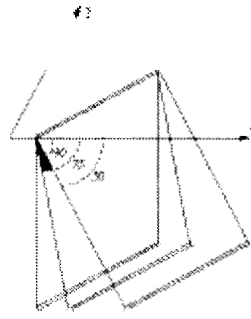


Figure 2 - Illustration of Dip Angle Variation

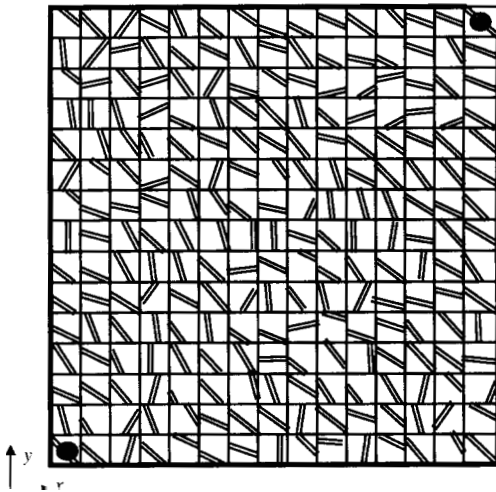


Figure 3 - Simulation Grid, with Random Fracture Orientation Variation by Fracture

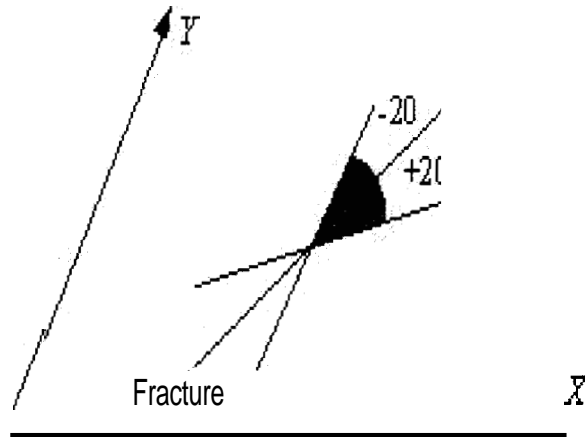


Figure 4 - Variation of Fracture Dip-Direction

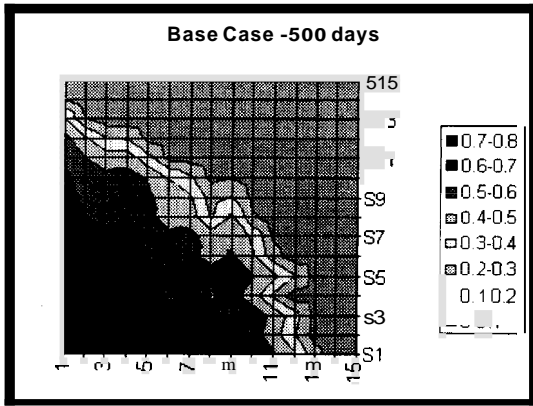


Figure 5 - Water Saturation Distribution at 500 Days

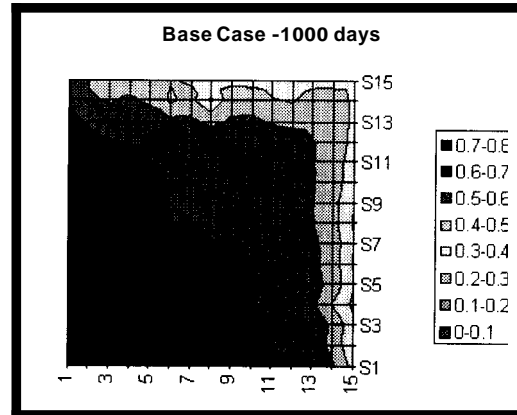


Figure 6 - Water Saturation Distribution at 1000 Days

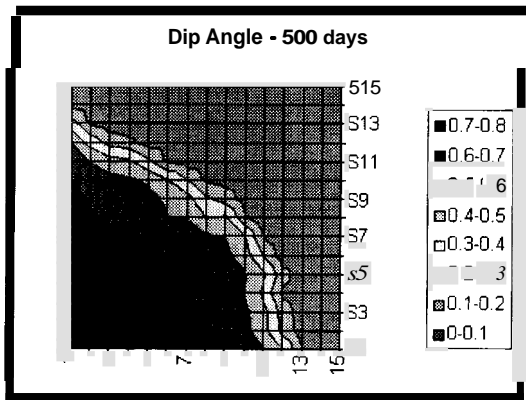


Figure 7 - Water Saturation Distribution at 500 Days

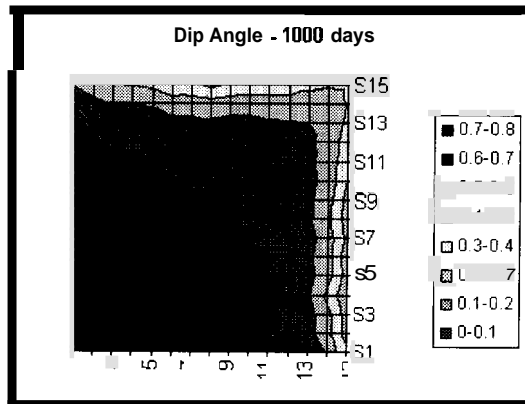


Figure 8 - Water Saturation Distribution at 1000 Days

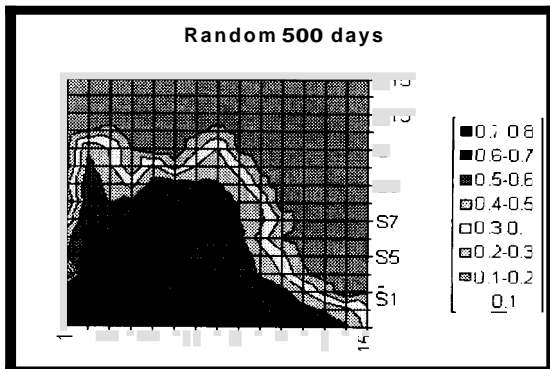


Figure 9 - Water Saturation Distribution at 500 Days

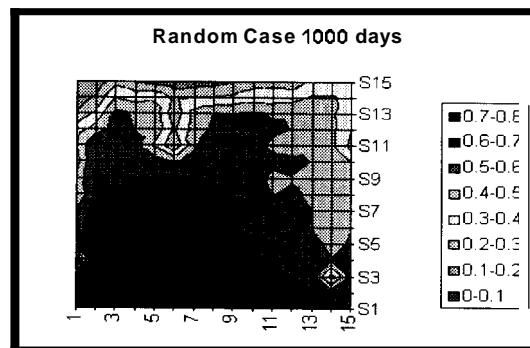


Figure 10 - Water Saturation Distribution at 1000 Days

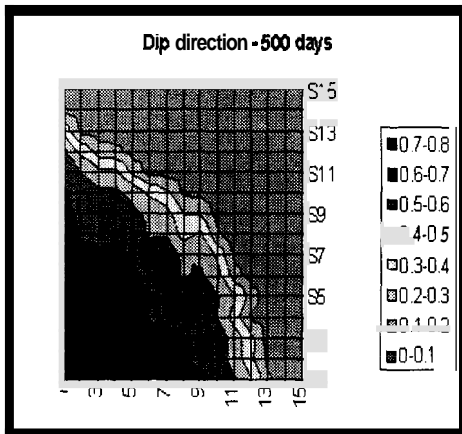


Figure 11 - Water Saturation Distribution at 500 Days

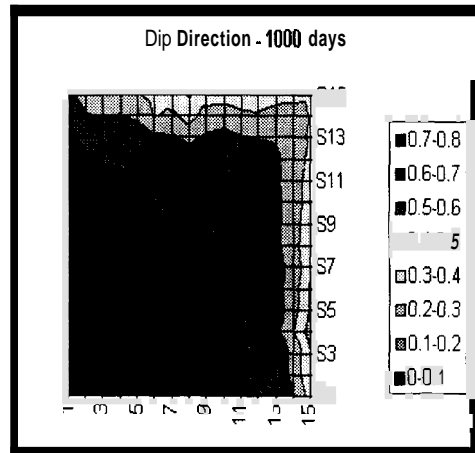


Figure 12 - Water Saturation Distribution at 1000 Days

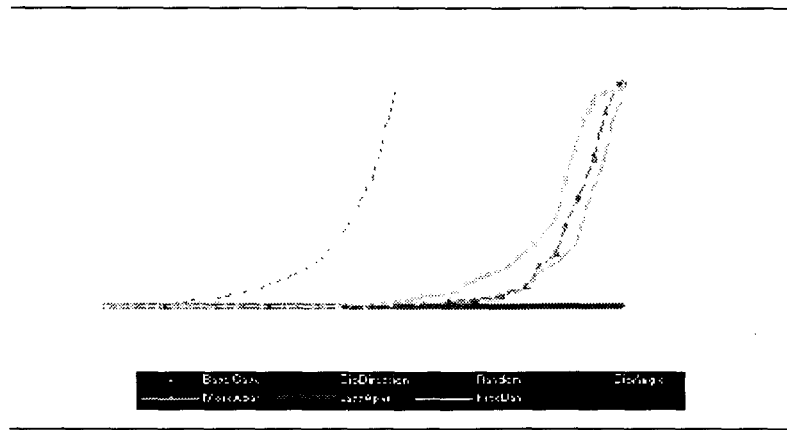


Figure 13 - Comparison of Water Production Predictions for Various Cases

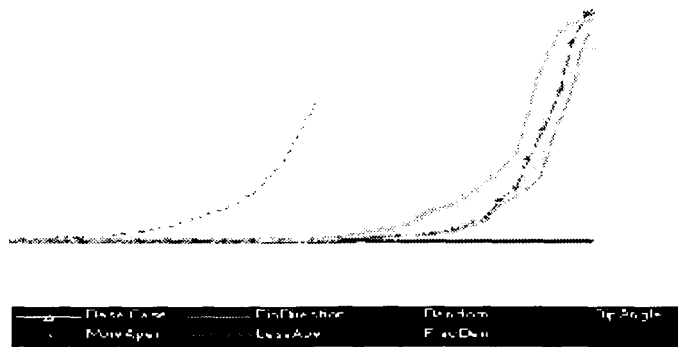


Figure 14 - Comparison of Water-Oil Ratio Predictions